JOURNAL OF MATERIALS SCIENCE 28 (1993) 2413–2422

Texture changes during superplastic deformation of mechanically alloyed aluminium IN90211

ZHE JIN, T. R. BIELER
Department of Materials Science and Mechanics, Michigan State University, East Lansing, MI 48824, USA

Superplastic deformation of mechanically alloyed aluminium IN90211 was studied by texture analysis. The textures in three deformed specimens were investigated as a function of strain using the three-dimensional crystal orientation distribution functions (CODFs). The results for the two superplastically deformed specimens (425 °C, strain rate of 1 s^{-1}, stress near 50 MPa, and 475 °C, initial strain rate of 77 s^{-1}, about 110 MPa) indicate that at strains below about 2.0, the specimen deforms by grain-boundary sliding and single (or double) slip, and at larger strains the deformation is dominated by grain-boundary sliding, multiple slip and some recrystallization. At 475 °C, 330 s^{-1}, and stress near 160 MPa, the specimen was above the superplastic regime, and the resulting texture changes with deformation were markedly different from superplastic results, and quite unusual.

1. Introduction

Superplastic deformation at high strain rates has been demonstrated in a number of materials, including IN90211 mechanically alloyed aluminium [1]. Texture evolution in superplasticity at low strain rates has been investigated. These studies generally show that texture decreases with increasing strain [2–6]. This can be explained by the randomizing effect that grain-boundary sliding has on grain orientations. Within some of these studies, certain components of texture associated with slip activity within the grains has been identified [2–5], but a consensus about the role of slip in superplasticity has not yet been reached.

Texture evolution at high strain rates was investigated using three deformed IN90211 specimens: a low- and a high-rate specimen within the superplastic regime, and a third at a rate above the superplastic regime. The implications of texture evolution on the role of slip and other deformation mechanisms will be discussed.

2. Experimental procedure

The material used in this study was IN90211; the composition is shown in Table I. The specimens were machined from a processed sheet which was extruded, forged and rolled at elevated temperature to a thickness of 2.5 mm. The sheet was annealed at 492 °C for 1 h and water quenched. Tensile specimens had the tensile axis parallel to the rolling direction. Details of the tensile experiments are found in [1]. The following specimens were studied: (1) true $\dot{\varepsilon} = 1\,s^{-1}$, $\sigma = 50$ MPa, $T = 425$ °C, superplastic; (2) initial $\dot{\varepsilon} = 77\,s^{-1}$, $\sigma = 110$ MPa, $T = 475$ °C, superplastic; (3) initial $\dot{\varepsilon} = 330\,s^{-1}$, $\sigma = 160$ MPa, $T = 475$ °C, not superplastic. The flow stress is high compared to other superplastic aluminium alloys. The deformed specimens were tapered, exhibiting strains between the maximum uniform true strain of about 1.0 to the fracture strain. The strain was determined from reduction of area assuming constant volume (cavitation is known to be less than 5% at the fracture surface [1]). Specimens were mounted and polished parallel to the rolling plane.

Texture measurements were carried out on a computer-controlled four-axis goniometer system in a Scintag diffractometer with a graphite monochrometer. Incomplete (1 1 1), (2 0 0), and (2 2 0) pole figures were made along the superplastically deformed specimen. The reflection method was used, with 5° azimuthal and 5° tilt increments up to a maximum tilt of 70°. A 1 mm diameter mask was used to limit the diffracted signal to the desired part of the specimen. Experimental pole figures were corrected and symmetrized prior to the crystal orientation distribution function (CODF) calculations using the preferred orientation package from Los Alamos (popLA, Los Alamos National Laboratory) [7].

3. Results

The CODF has the advantage of being a unique description of texture compared to pole figures and inverse pole figures. Changes in texture as a function of strain are presented together for the two superplastic specimens and briefly for the non-superplastic Region III specimen.

3.1. Superplastic deformation (Region II)

The complete experimental CODFs obtained from the specimens deformed in Region II of superplastic deformation ($\dot{\varepsilon} = 1\,s^{-1}$ at $T = 425$ °C and $\dot{\varepsilon} = 77\,s^{-1}$ at $T = 475$ °C) are shown at sections of constant ϕ in Figs

TABLE I Composition (wt %) of IN90211

Mg	Cu	C	O	Al_2Cu	Al_4C_3	Al_2O_3	Al
2.0	4.4	1.1	0.8				91.7
[a] 2.0	0.9			6.4	4.3	1.7	84.7
[a]				4.1 vol %	4.1 vol %	1.2 vol %	90.6 vol %

[a] Assuming 80% Cu in Al_2Cu, O and C in Al_2O_3 and Al_4C_3, and Mg in solution.

1 and 2, respectively. We are mainly considering the fibre-type texture in $\phi = 0°$ section of the CODF and some specific peak type components in the sections from the whole range of ϕ.

The initial texture was not the same for each specimen (due to variations in the forging and rolling history of the sheet). The initial texture in the undeformed shoulder mainly consists of three fibre textures: (1 0 1) [*u v w*] (α-fibre texture), (1 0 2) [*u v w*] and (2 0 1) [*u v w*]. Because the latter two textures are symmetric about $\theta = 45°$ in the $\phi = 0°$ section, only the components of (1 0 2) [*u v w*] texture will be considered below. In the specimen deformed at $\dot{\varepsilon} = 77\,s^{-1}$ there are also very high intensities at (2 0 3) [$\bar{3}$ 0 2] and (3 1 1) [0 $\bar{1}$ 1]. But there are no (0 0 1) [1 0 0] cube components in either initial texture.

For the specimen deformed at $\dot{\varepsilon} = 1\,s^{-1}$ and $T = 425\,°C$, the intensity in the α-fibre decreases with strain until $\varepsilon = 1.6$ and increases thereafter, but the overall texture decreases with respect to the initial α-fibre texture (Fig. 3a). In the (1 0 2) [*u v w*] fibre, the overall intensity remains constant even though individual components change with strain (Fig. 3b). At $\varepsilon = 3.0$, near the fracture tip, a new fibre (*h* 0 1) [0 1 0] developed and a strong cube texture emerged (Fig. 1f).

For the specimen deformed at $\dot{\varepsilon} = 77\,s^{-1}$ and $T = 475\,°C$, the intensity in the α-fibre remains unchanged at low strain, but at $\varepsilon > 2.13$, the components from (1 0 1) [0 $\bar{1}$ 0] to (1 0 1) [$\bar{2}$ $\bar{3}$ 2] are sharpened and the previous high-intensity components from (1 0 1) [$\bar{1}$ $\bar{1}$ 1] to (1 0 1) [$\bar{1}$ 0 1] are weakened (Fig. 4a). The overall intensity in the (1 0 2) [*u v w*] fibre decreases (Fig. 4b). Several new texture components are noted at high strain in this specimen. At $\varepsilon = 2.13$, peak-type components (3 1 2) [$\bar{1}$ $\bar{1}$ 2], (3 2 1) [$\bar{1}$ $\bar{4}$ 11], (2 3 1) [4 $\bar{3}$ 1], (1 2 3) [$\bar{1}$ $\bar{4}$ 3] and (1 3 2) [1 $\bar{3}$ 4] and a cube texture are developed (Fig. 2c). At $\varepsilon = 2.36$, the formerly developed (3 2 1) [$\bar{1}$ $\bar{4}$ 11] is shifted to (3 2 1) [$\bar{2}$ $\bar{3}$ 12] and a new peak (3 2 1) [1 $\bar{2}$ 1] develops, while the former peaks (3 1 2) [$\bar{1}$ $\bar{1}$ 2], (2 3 1) [4 $\bar{3}$ 1], (1 2 3) [$\bar{1}$ $\bar{4}$ 3] and (1 3 2) [1 $\bar{3}$ 4] are weakened. It is also noted that a new fibre texture (1 1 3) [*u v w*] is developed with a maximum intensity at (1 1 3) [0 $\bar{3}$ 1] (Fig. 2d). At $\varepsilon = 2.86$, a new orientation $\langle 0\,2\,3\rangle \| RD$ (the rolling direction), such as (11 2 3) [0 $\bar{3}$ 2], (12 3 2) [0 $\bar{2}$ 3], (8 2 3) [0 $\bar{3}$ 2], (3 2 11) [2 $\bar{3}$ 0] and (3 2 12)

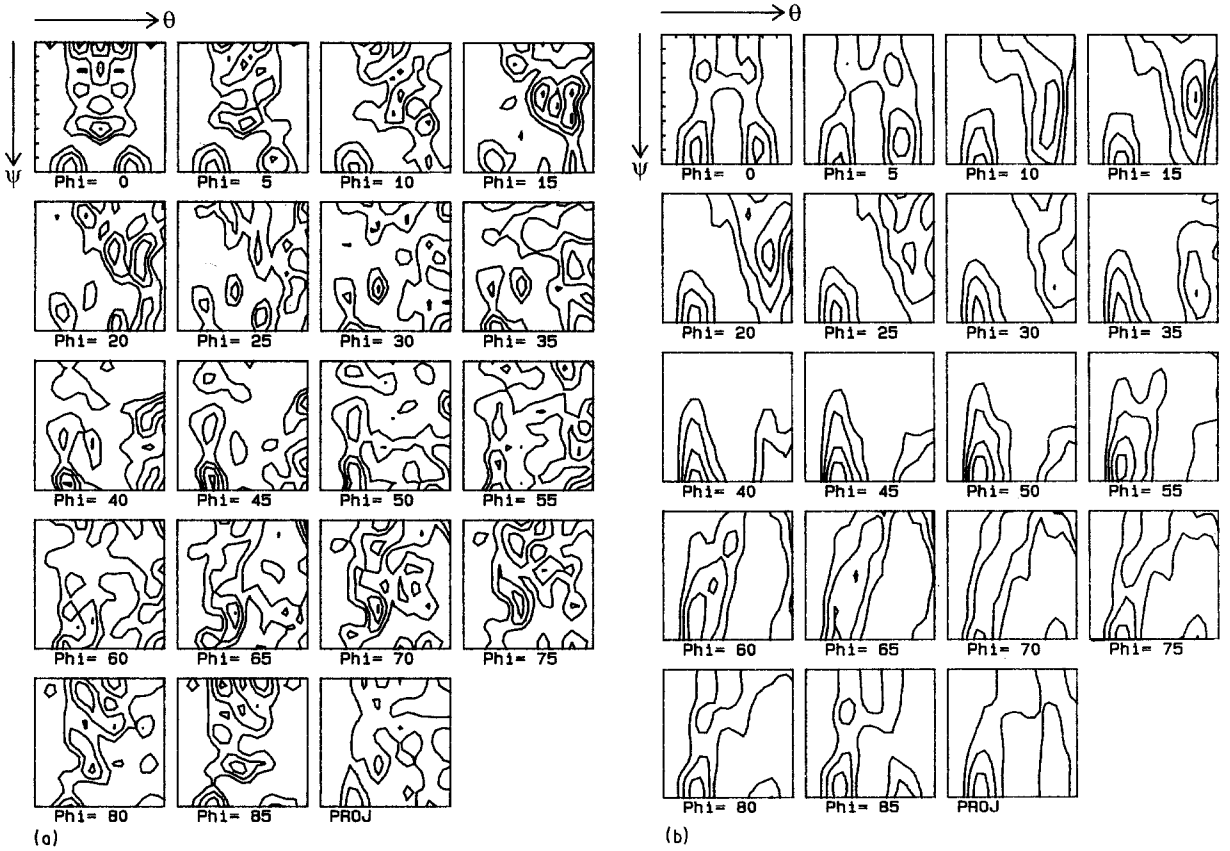

Figure 1 Complete experimental CODF of specimen deformed at $\dot{\varepsilon} = 1\,s^{-1}$ and $T = 425\,°C$. (a–f) Strain and contour levels: (a) $\varepsilon = 0$ (1 2 3 4), (b) $\varepsilon = 1.1$ (1 2 3 4 5), (c) $\varepsilon = 1.6$ (1 2 3), (d) $\varepsilon = 2.3$ (1 2 3), (e) $\varepsilon = 2.6$ (1 2 3 4), (f) $\varepsilon = 3.0$ (1 2 3 4).

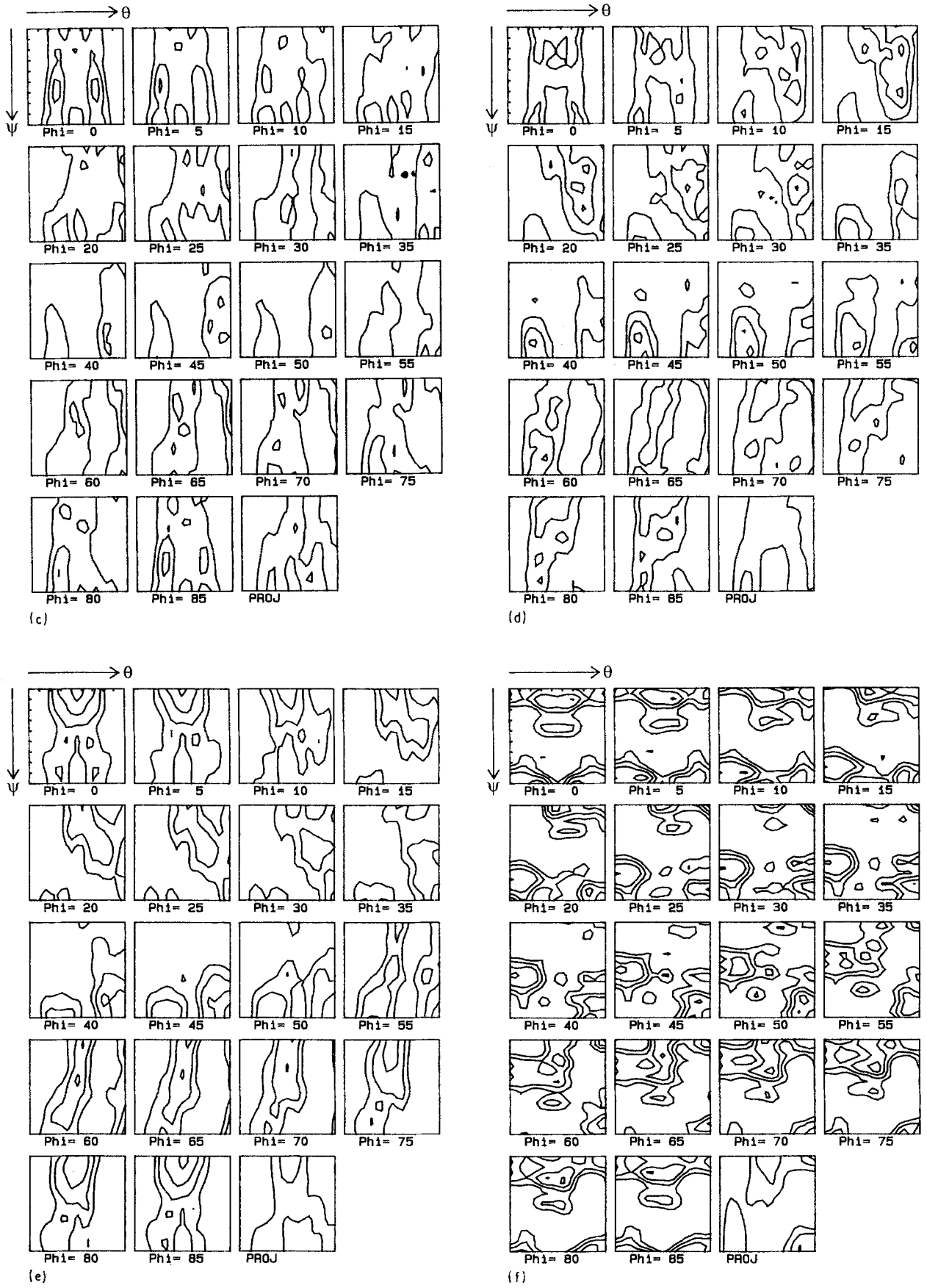

Figure 1 Continued

[2 $\bar{3}$ 0], is strongly developed even though the peak (2 0 3) [$\bar{3}$ 0 2] reaches minimum intensity compared to that at low strain. New strong peaks (6 1 1) [$\bar{1}$ $\bar{6}$ 12] and (1 1 6) [6 $\bar{12}$ 1] are also created (Fig. 2e).

3.2. Non-superplastic deformation (Region III)

The complete experimental CODFs of this specimen are shown in Fig. 5. In this specimen, two fibre

textures, which are different from those in other two specimens, are found: one is (2 0 3) [$u\,v\,w$] and the other is a skeleton line in which the [0 0 1] orientation is tilted from ND towards TD by about 30°. The results are plotted in Fig. 6. The overall intensity of the skeleton line remains constant until $\varepsilon = 1.38$, where some parts of the skeleton line are sharpened slightly (Fig. 6a). But, the overall intensity of the fibre (2 0 3) [$u\,v\,w$] decreases with increasing strain (Fig. 6b).

4. Analysis and discussion

4.1. Superplastic deformation (Region II)

The textures of specimens deformed at $\dot{\varepsilon} = 1$ and

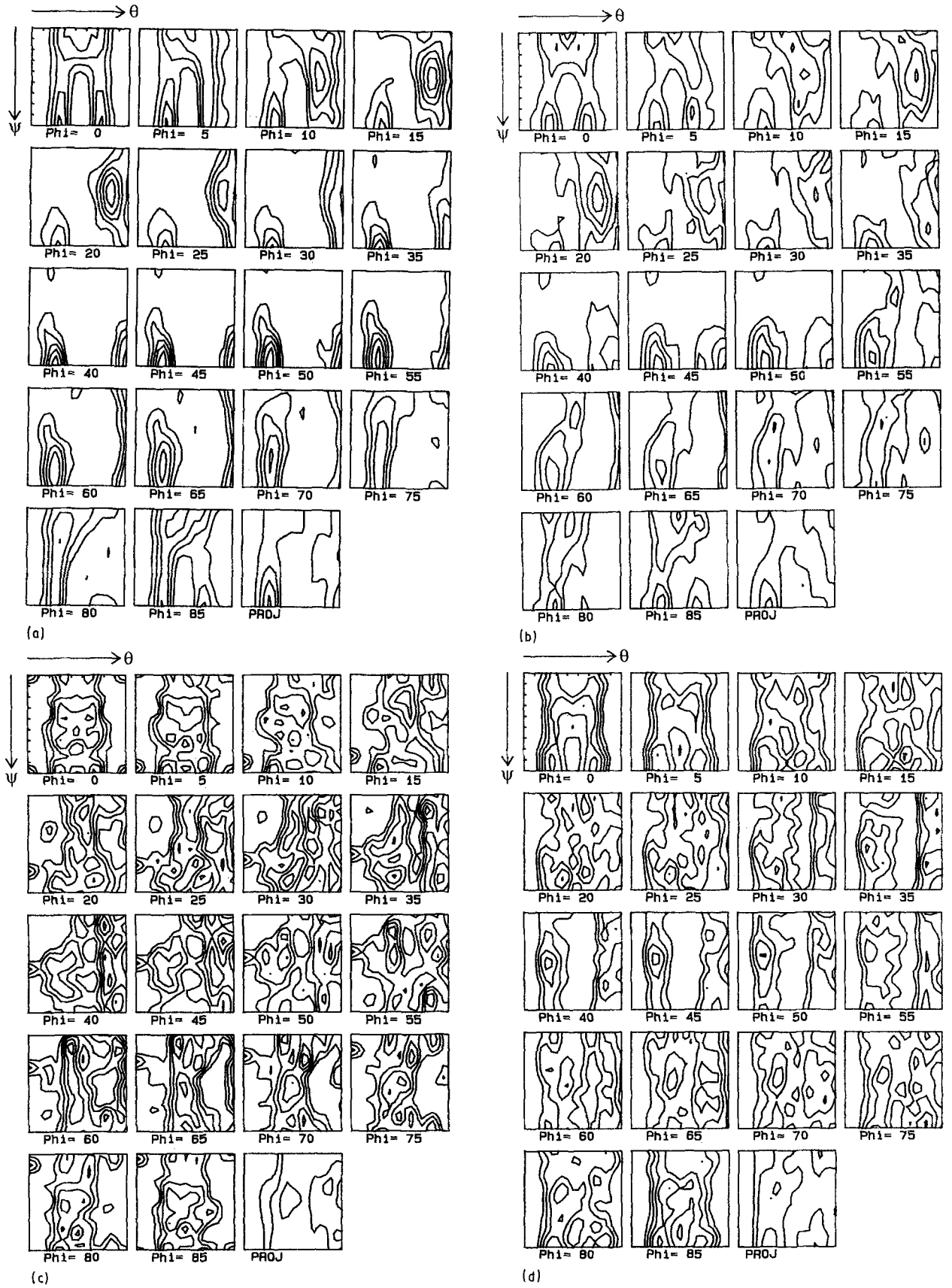

Figure 2 Complete experimental CODF of specimen deformed at $\dot{\varepsilon} = 77\,s^{-1}$ and $T = 475\,°C$. (a–e) Strain and contour levels: (a) $\varepsilon = 0$ (1 2 3 4 5), (b) $\varepsilon = 1.6$ (1 2 3 4), (c) $\varepsilon = 2.13$ (0.5 1 1.5 2 2.5), (d) $\varepsilon = 2.36$ (0.5 1 1.5 2 2.5), (e) $\varepsilon = 2.86$ (1 2 3 4 5).

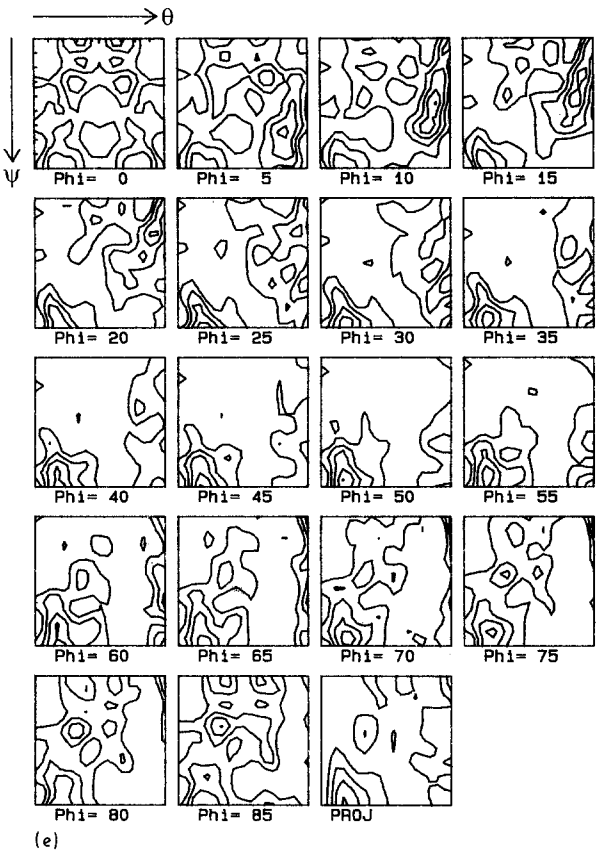

Figure 2 Continued

77 s^{-1}, are mainly composed of two fibre textures, with ⟨1 0 1⟩ and ⟨1 0 2⟩ directions parallel to the rolling plane normal, and some individual peaks. During the superplastic deformation, two fibre textures dominate the texture components, even though the intensities of individual components in these fibres change with strain. The texture changes produced by superplastic deformation can be described in terms of grain-boundary sliding, slip and dynamic recrystallization.

4.1.1. Grain-boundary sliding

In Fig. 7, some ideal components are plotted versus strain. The overall texture intensity decreases with strain up to $\varepsilon = 2.6$ in the first specimen and $\varepsilon = 2.13$ in the second specimen.

The texture decrease in superplastic deformation cannot be explained in terms of slip or recrystallization, because annealing is found to lead to only a slight or no reduction in intensity and recrystallization leads to the development of new and distinct texture components. However, this overall reduction can be easily accounted for in terms of grain-boundary sliding (GBS) and grain rotation. The mechanism of GBS for this material is schematically shown in Fig. 8 [1]. Because the grain aspect ratio is about 1–10, the sliding in the direction perpendicular to the plane of the grain is difficult. The GBS and grain rotation take place in the plane parallel to the rolling plane, and the grains remain in the same plane as they started. Grain-boundary sliding and grain rotation have a randomizing effect on any existing texture components [2–5]. However, the randomizing effect of GBS and grain rotation in these specimens is restricted in the direction perpendicular to the rolling plane due to the plate shape of the grains. Therefore, the sliding stresses on the different types of boundaries are accommodated by either grain rotation in the rolling plane or dislocation slip in grain interiors, as shown in Fig. 8. The

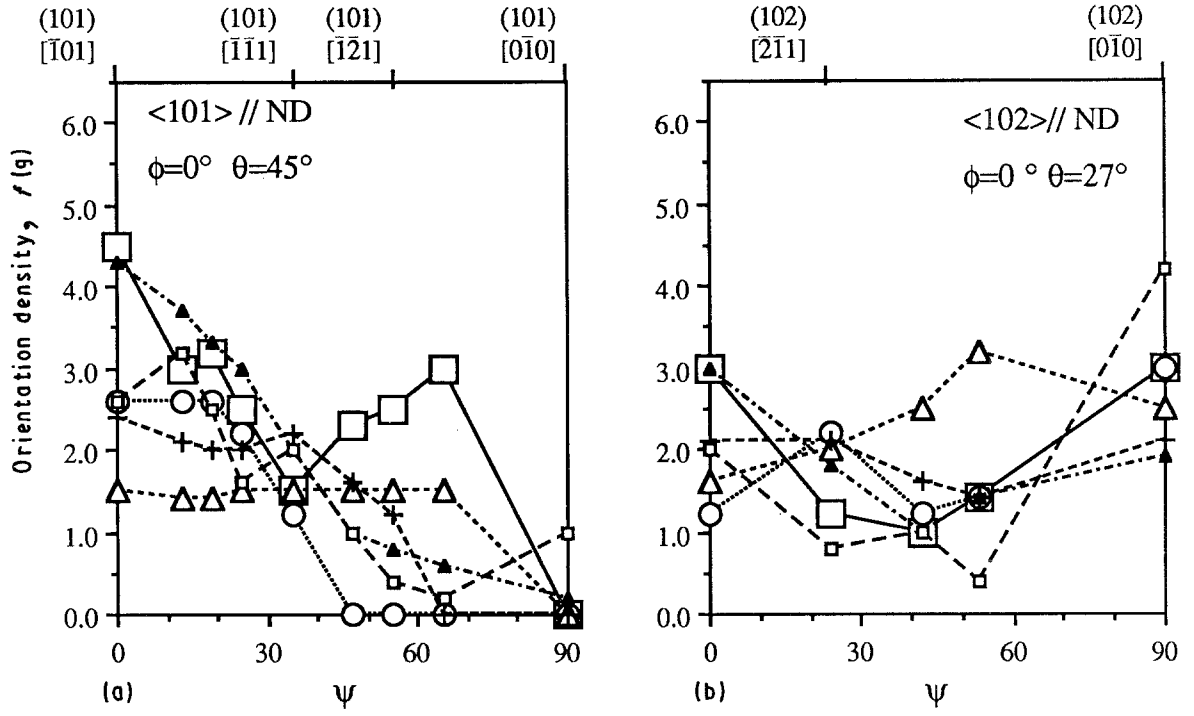

Figure 3 Orientation density of (a) α-fibre and (b) (1 0 2) [*u v w*] fibre of specimen deformed at $\dot{\varepsilon} = 1\ s^{-1}$ and $T = 425\,°C$ versus strain: (□) 0, (○) 1.1, (△) 1.6, (+) 2.3, (▲) 2.6, (▫) 3.0.

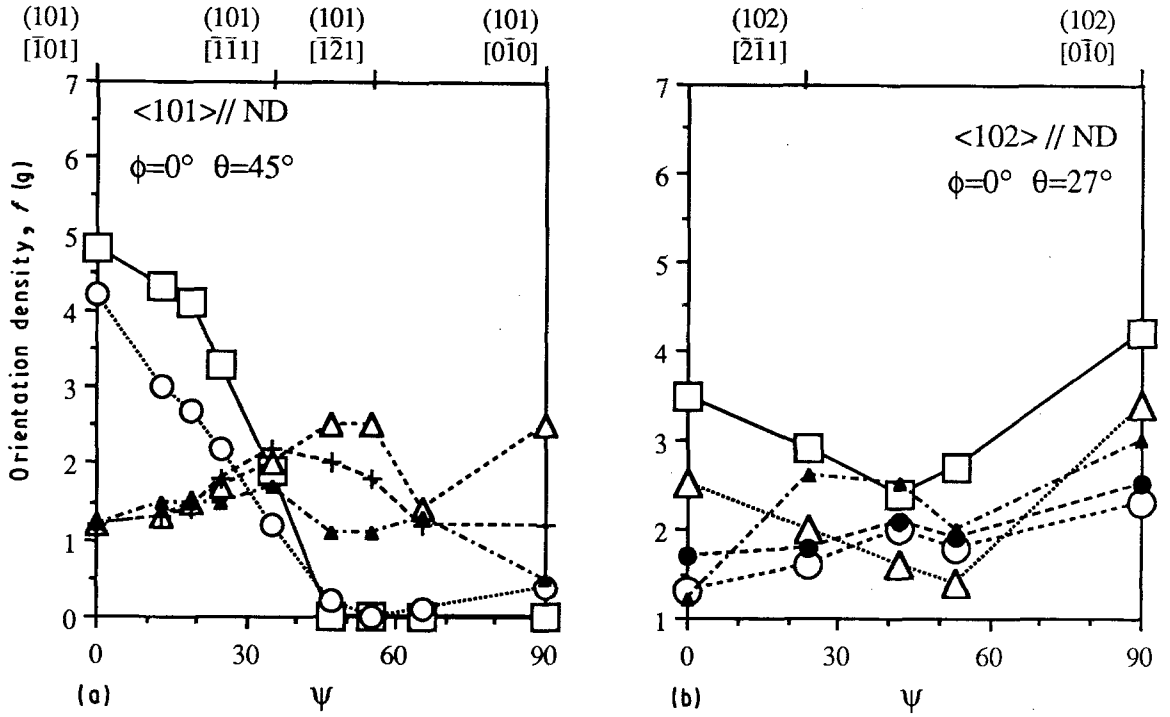

Figure 4 Orientation density of (a) α-fibre and (b) (1 0 2) [*u v w*] fibre of specimen deformed at $\dot{\varepsilon} = 77\ s^{-1}$ and $T = 475\,°C$ versus strain: (□) 0, (○) 1.6, (△) 2.13, (+) 2.36, (▲) 2.86.

relatively slow reduction of overall texture intensity implies that the grain rotation rate is limited. But it is difficult to make a quantitative assessment of the contribution of the rotation rate to an individual orientation, because there are concurrent sharpening and weakening of existing texture components due to the occurrence of slip and recrystallization.

4.1.2. Slip

Investigation of the [$\bar{2}\,\bar{1}$ 1] orientation in Fig. 7 shows the occurrence of single slip during superplastic deformation. In Fig. 7a, the intensity of [$\bar{2}\,\bar{1}$ 1] orientation is relatively high at low strain, and it drops with increasing strain. However, in Fig. 7b for the higher rate, the intensity of the [$\bar{2}\,\bar{1}$ 1] orientation continues to increase after an initial drop of overall intensity due to GBS and grain rotation. It is possible to treat a grain as an isolated single crystal in uniaxial tension in the case of diffusion-accommodated superplastic deformation, so that the single slip allows the grain to rotate to a ⟨1 2 1⟩ direction where the second slip system operates and keeps the grain at ⟨1 2 1⟩. Furthermore, ⟨1 2 1⟩ orientations have a relatively high Schmid factor (0.41) and thus slip is probable in grains at or near these orientations [6]. The sharpening of the [$\bar{2}\,\bar{1}$ 1] orientation indicates that a large amount of single slip has occurred. The reduction of the [$\bar{2}\,\bar{1}$ 1] orientation with further strain may be attributed to an increase in the number of grains with multiple slip and the occurrence of dynamic recrystallization in the lower strain-rate specimen. The increment of [$\bar{2}\,\bar{1}$ 1] orientation with strain in Fig. 7b indicates more single slip occurs at high strain. Such an orientation is stable in the sense that any rotation away from it occasioned by GBS leads to a counteracting slip rotation back towards ⟨1 2 1⟩.

The gradual increase of a [$\bar{1}\,\bar{1}$ 1] orientation suggests that multiple slip occurs in this specimen because the ⟨1 1 1⟩ texture is commonly associated with multiple slip under uniaxial tension in polycrystalline materials [8]. The ⟨1 1 1⟩ texture is stable during multiple slip, because only five of the six active slip systems in this orientation are required to maintain grain compatibility and the remaining one degree of freedom allows a rotation of the grains about the tensile axis only [9].

There are strong ⟨1 0 0⟩ components in the starting materials, compared to the other texture components, but the ⟨1 0 0⟩ texture gradually declines up to $\varepsilon = 2.6$ at $\dot{\varepsilon} = 1\ s^{-1}$ (see Fig. 7a) and $\varepsilon = 2.13$ at $\dot{\varepsilon} = 77\ s^{-1}$ (see Fig. 7b). This is because the ⟨1 0 0⟩ orientation has eight active slip systems, so that after providing five slip systems for grain compatibility, the grain still has three degrees of freedom and any rotation is possible [9]. Close to the fracture surface in the specimen deformed at $\dot{\varepsilon} = 1\ s^{-1}$, where neck formation and a rising local temperature take place [1], and also at the higher strains in the specimen deformed at $\dot{\varepsilon} = 77\ s^{-1}$, the dominant slip system shifts from ⟨1 1 1⟩ to ⟨1 0 0⟩ directions. The ⟨1 0 0⟩ orientation is apparently more likely to operate at larger strains in this material. This may be related to the effect of increasing temperature from adiabatic heating, and its possible effect of decreasing boundary constraints due to increased boundary diffusivity. In this case the deformation in each grain is more like that of an isolated single crystal in uniaxial tension [10]. Further, the Schmid factors for the ⟨1 0 0⟩ and ⟨1 1 1⟩ orientations are 0.408 and 0.272, respectively. This leads to increasing intensity in the ⟨1 0 0⟩ orientation.

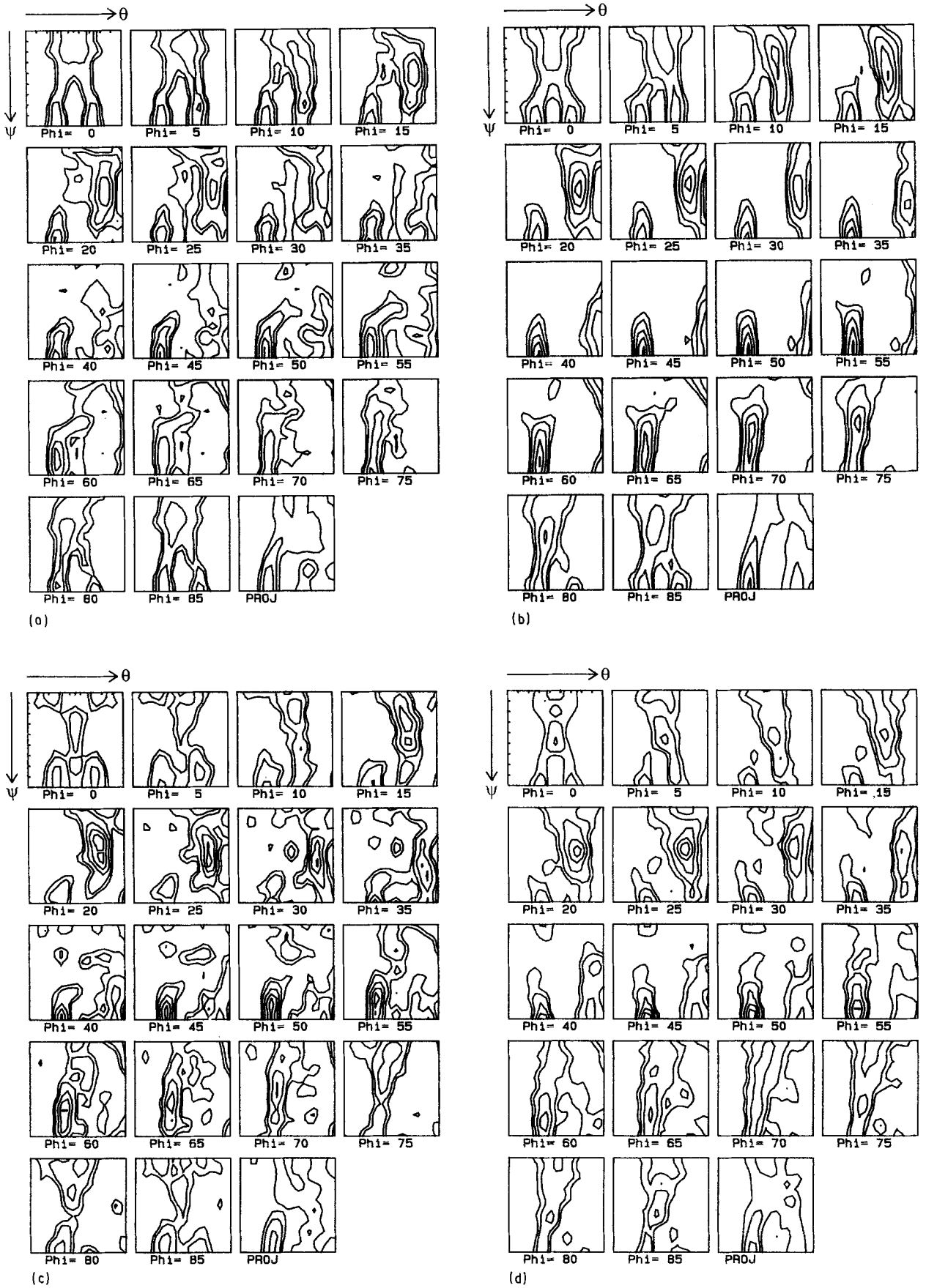

Figure 5 Complete experimental CODF of specimen deformed at $\dot{\varepsilon} = 330\,s^{-1}$ and $T = 475\,°C$. (a–d) Strain and contour levels: (a) $\varepsilon = 0$ (1 2 4 6 8), (b) $\varepsilon = 0.45$ (1 2 4 6 8), (c) $\varepsilon = 0.73$ (1 2 4 6 8), (d) $\varepsilon = 1.38$ (1 2 4 6 8).

4.1.3. Recrystallization

The appearance of cube texture at the highest strain in the specimen deformed at $1\,s^{-1}$ and at a median strain in the specimen deformed at $77\,s^{-1}$ suggests that recrystallization occurs. The small amount of this component is possibly due to the effects of the finely dispersed particles and fine substructures. The deformation zone at large particles is a preferred nucleation

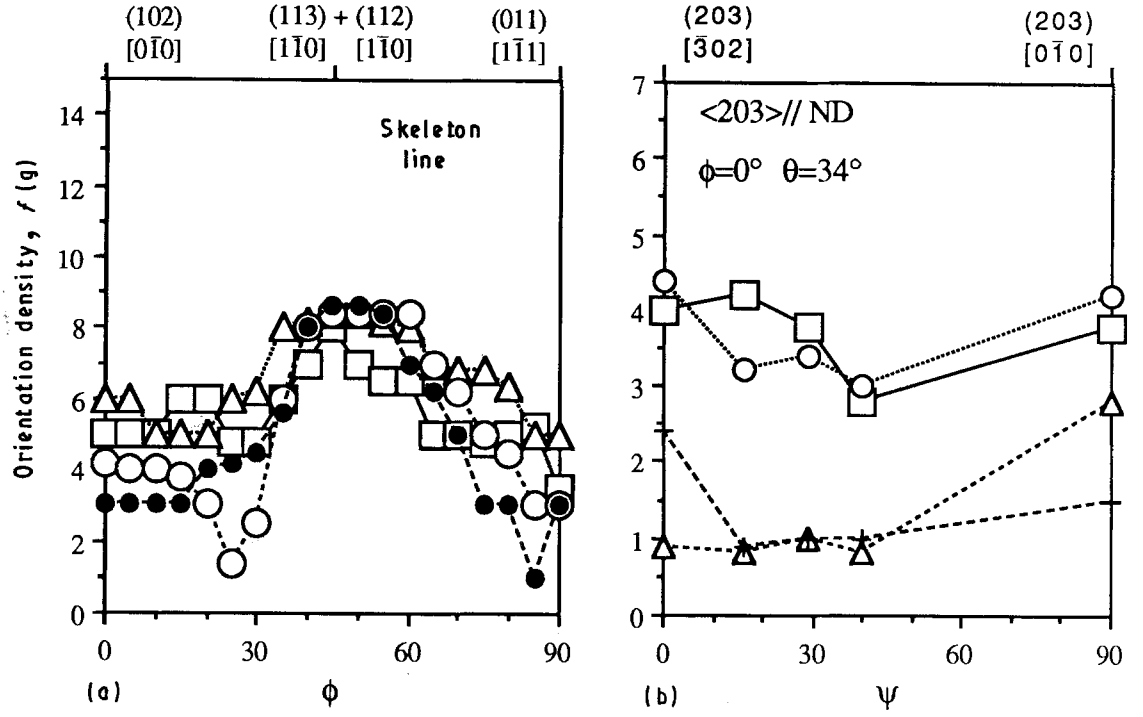

Figure 6 Orientation density of (a) skeleton line and (b) (2 0 3) [*u v w*] of specimen deformed at $\dot{\varepsilon} = 330\,s^{-1}$ and $T = 475\,°C$ versus strain: (a) (□) 0, (△) 0.45, (○) 0.723, (●) 1.38; (b) (□) 0, (○) 0.45, (△) 0.72, (+) 1.38.

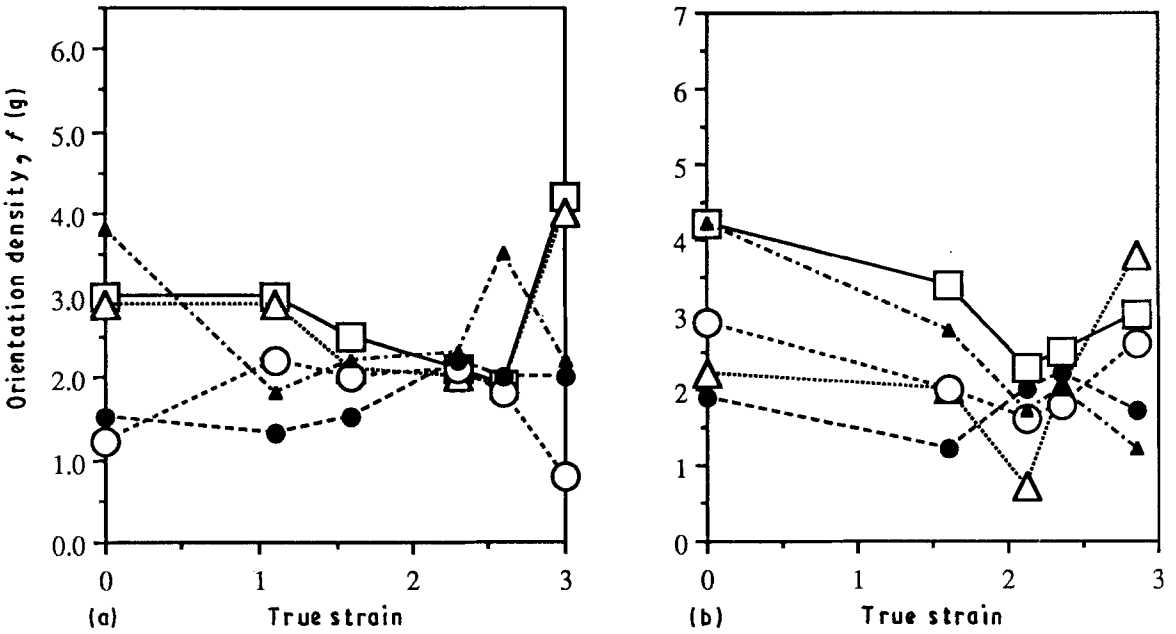

Figure 7 Some texture components versus true strain for the superplastically deformed specimens. (a) $1\,s^{-1}$, 425 °C, (b) $77\,s^{-1}$, 475 °C. (□) (1 0 2) [0 $\bar{1}$ 0], (△) (1 0 3) [0 $\bar{1}$ 0], (○) (1 0 2) [$\bar{2}$ $\bar{1}$ 1]; (●) (1 0 1) ($\bar{1}$ $\bar{1}$ 1), (▲) (2 0 3) [$\bar{3}$ 0 2].

site for recrystallization. Therefore, the contribution of the particles to the overall texture is expected to be a smearing out of the deformation texture by an amount which depends on the volume fraction of particles present [11–15]. However, for small particles ($< 0.1\,\mu m$), some studies have shown that the texture is strengthened, whereas in other cases a neutral or a weakening effect has been observed [16–18]. In this study, because the particle size is very small (10–35 nm) and the spacing between the particles is 40 nm, the particles have such a strong pinning effect on both substructures and grain boundaries that subgrains are very difficult to grow into a recrystallizing nucleus. So a large strain is required to overcome this barrier for recrystallization. This result may also be related to an effect of particles on the formation of dynamic recrystallization nuclei at the original grain boundaries [19]. The nucleation process is retarded by presence of small particles. This retarding effect may be less pronounced at the original grain boundaries where nucleation may require less subgrain growth than nucleation in the grain interiors. The

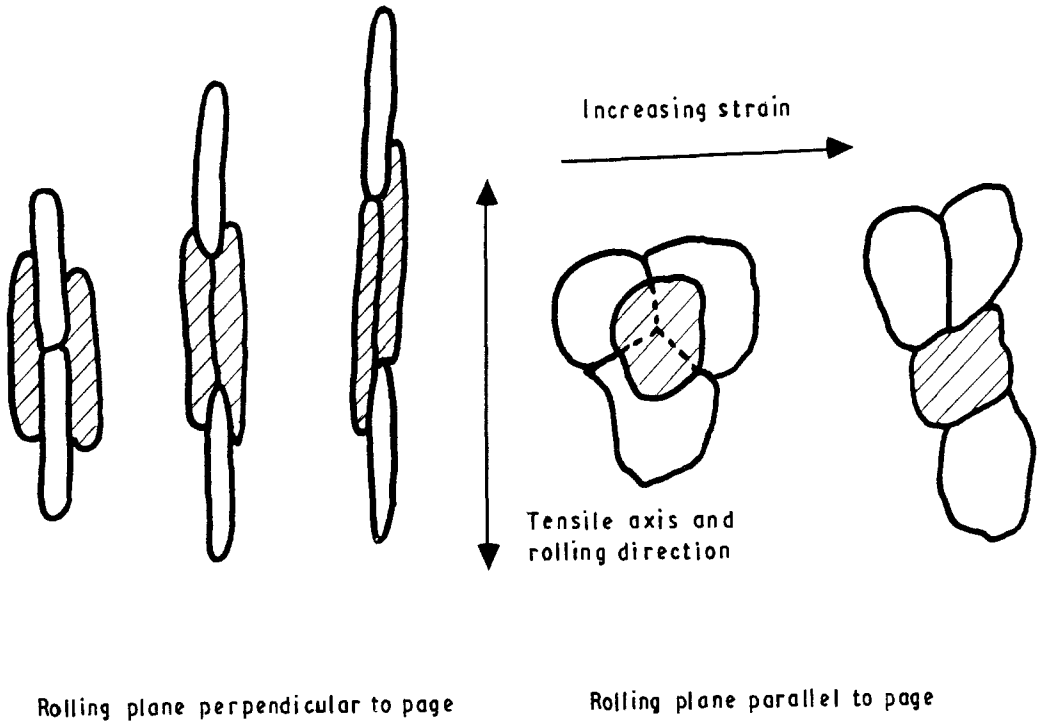

Figure 8 Schematic diagram showing sliding of platelet-shaped grains during superplastic elongation.

preference for nucleation at the original grain boundaries may lead to an increased retention of the initial texture [20, 21].

4.2. Non-superplastic deformation (Region III)

The specimen deformed at $\dot{\varepsilon} = 330\,s^{-1}$ mainly consists of one skeleton fibre texture which runs from (1 0 2) [0 $\bar{1}$ 0] to (0 1 1) [1 $\bar{1}$ 1]. Contrary to the overall reduction of intensity in the superplastically deformed specimen, the overall intensity in this specimen remains constant. Therefore, there should be some kind of balance between sharpening and weakening effects due to slip, recrystallization, GBS and grain rotation. In this specimen, components of (1 0 2) [0 $\bar{1}$ 0] and (0 1 1) [1 $\bar{1}$ 1] decrease in intensity with strain, while the intensities of (1 1 3) [1 $\bar{1}$ 0] and (1 1 2) [1 $\bar{1}$ 0] components increase as strain increases. This result is contrary to the traditional deformation mechanism which predicts an increment of ⟨0 0 1⟩ and ⟨1 1 1⟩ orientations by tensile deformation. It indicates that an unusual deformation mechanism is occurring and the superplastic deformation mechanisms described above are no longer dominant.

5. Conclusions

1. The superplastic deformation mechanism of IN90211 consists of grain-boundary sliding, dislocation slip (single slip and multiple slip), grain rotation and recrystallization.

2. Recrystallization components are weak and only seen after a large amount of strain. At the highest strain rate, where less strain occurred, there is no evidence of recrystallization.

3. At the lower strain rates ($1\,s^{-1}$ and $77\,s^{-1}$), the textures are dominated by two fibres, α-fibre (⟨1 0 1⟩ parallel to ND) and {1 0 2}⟨*u v w*⟩ (⟨1 0 2⟩ parallel to ND). At the highest strain rate ($330\,s^{-1}$), the textures are mainly composed of two fibres, {2 0 3} ⟨*u v w*⟩ (⟨2 0 3⟩ parallel to ND) and a skeleton line (⟨0 0 1⟩ orientation is tilted from ND towards TD by about 30°).

Acknowledgements

The authors thank Dr U. F. Kocks, Los Alamos National Laboratories, for his help in the use of popLA. Partial support for this work came from a research initiation grant from Michigan State University.

References

1. T. R. BIELER, G. R. GOTO and A. K. MUKHERJEE, *J. Mater. Sci.* **25** (1990) 4125.
2. K. N. MELTON, C. P. CUTLER, J. S. KALLEND and J. W. EDINGTON, *Acta Metall.* **22** (1974) 165.
3. C. P. CUTLER, J. W. EDINGTON, J. S. KALLEND and K. N. MELTON, *ibid.* **22** (1974) 665.
4. *Idem, Metal Sci. J.* **5** (1971) 210.
5. K. N. MELTON, C. P. CUTLER and J. W. EDINGTON, *Scripta Metall.* **8** (1974) 1141.
6. K. MATSUKI, H. MORITA, M. YAMADA and Y. MURAKAMI, *Metal Sci.* **11** (1977) 156.
7. J. S. KALLEND, U. F. KOCKS, A. D. ROLLETT and H.-R. WENK, *Mater. Sci. Engng* **A132** (1991) 1.
8. I. L. DILLAMORE and W. T. ROBERTS, *Metall. Rev.* **10** (1965) 271.
9. U. F. KOCKS, *Metall. Trans.* **1** (1970) 1121.
10. G. Y. CHIN, in "Texture in Research and Practice", edited by G. Wassermann and J. Grewen (Springer, Berlin, 1969) p. 51.
11. F. J. HUMPHREYS, *Acta Metall.* **27** (1979) 1801.
12. *Idem, ibid.* **25** (1977) 1323.

13. P. HERBST and J. HUBER, in "Textures of Materials", edited by G. Gottstein and K. Lucke (Springer, Berlin, 1978) p. 453.
14. P. N. KALU and F. J. HUMPHREYS, in "8th International Conference on Textures of Materials", Santa Fe, New Mexico, edited by J. S. Kallend and G. Gottstein (The Metallurgical Society, Warrendale, Pa, 1987) p. 511.
15. D. JUUL JENSEN, N. HANSEN and F. J. HUMPHREYS, *ibid.*, p. 431.
16. N. HANSEN and D. JUUL JENSEN, in "Annealing Processes-Recovery, Recrystallization and Grain Growth", edited by N. Hansen, D. Juul Jensen, T. Leffers and B. Ralph (RISØ National Laboratory, Roskilde, 1986) p. 337.
17. R. GARVIN-SALAZAR, M. BRABERS and E. AERNOUDT, *Mater. Sci. Engng* **26** (1976) 251.
18. G. BONISSONI and M. PAGANELLI, *Appl. Mater. Res.* **4** (1965) 84.
19. N. HANSEN and B. BAY, *Acta Metall.* **29** (1981) 65.
20. G. L. FERRAN, R. D. DOHERTY and R. W. CAHN, *ibid.* **19** (1971) 1019.
21. N. HANSEN and D. JUUL JENSEN, *Metall. Trans.* **17A** (1986) 253.

Received 5 February
and accepted 12 October 1992